
FineMolTex: Towards Fine-grained Molecular Graph-Text Pre-training

Yibo Li*

Beijing University of Posts
and Telecommunications, China
yiboL@bupt.edu.cn

Yuan Fang[†]

Singapore Management University, Singapore
yfang@smu.edu.sg

Mengmei Zhang

China Telecom Bestpay, China
zhangmengmei@bestpay.com.cn

Chuan Shi[†]

Beijing University of Posts
and Telecommunications, China
shichuan@bupt.edu.cn

Abstract

Understanding molecular structure and related knowledge is crucial for scientific research. Recent studies integrate molecular graphs with their textual descriptions to enhance molecular representation learning. However, they focus on the whole molecular graph and neglect frequently occurring subgraphs, known as motifs, which are essential for determining molecular properties. Without such fine-grained knowledge, these models struggle to generalize to unseen molecules and tasks that require motif-level insights. To bridge this gap, we propose FineMolTex, a novel **Fine-grained Molecular graph-Text** pre-training framework to jointly learn coarse-grained molecule-level knowledge and fine-grained motif-level knowledge. Specifically, FineMolTex consists of two pre-training tasks: a contrastive alignment task for coarse-grained matching and a masked multi-modal modeling task for fine-grained matching. In particular, the latter predicts the labels of masked motifs and words, leveraging insights from each other, thereby enabling FineMolTex to understand the fine-grained matching between motifs and words. Finally, we conduct extensive experiments across three downstream tasks, achieving up to 230% improvement in the text-based molecule editing task. Additionally, our case studies reveal that FineMolTex successfully captures fine-grained knowledge, potentially offering valuable insights for drug discovery and catalyst design.

1 Introduction

Comprehending molecular structure and related knowledge is pivotal in scientific investigations spanning diverse fields, including chemistry, drug discovery, and materials science [11]. Recent advancements in artificial intelligence and machine learning have yielded promising outcomes for molecule-based tasks such as retrosynthesis [47] and drug discovery [11]. The majority of these studies [17, 7, 24, 38, 1] concentrate on the molecular structure, such as SMILES strings, molecular graphs, and geometric structures. They learn molecular representations under supervised signals such as toxicity level and drug activity. However, this type of supervised learning requires extensive and costly labeling of pre-defined categories, hindering its adoption for unseen categories and tasks.

Fortunately, compared to task-specific labeled data, textual descriptions of molecules are fairly abundant. These descriptions can be found in chemical database annotations, research papers in

*This work was done when the first author was a visiting student at Singapore Management University.

[†]Corresponding authors.

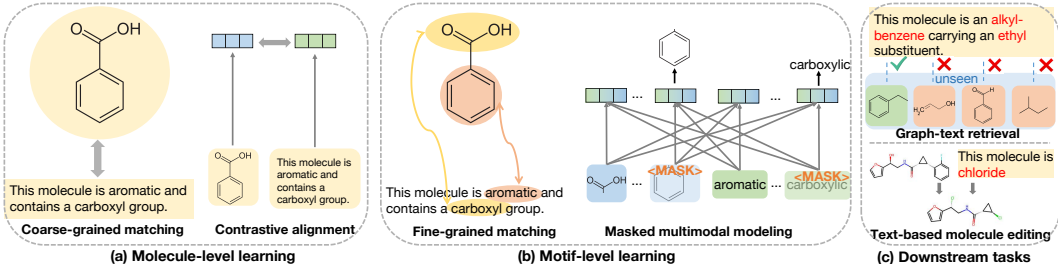


Figure 1: Comparison of molecule- and motif-level learning, and illustration of downstream tasks.

chemistry and biology, and drug instruction sheets [26], providing general information on molecular usage, efficacy, chemical properties, and even detailed insights into specific functional groups and chemical moieties [16]. Hence, several studies explore molecular structures along with their corresponding descriptions. MoleculeSTM [26] and MoMu [35] align the whole molecular graphs with their textual descriptions employing a contrastive learning approach as shown in Figure 1(a). MolCA [27] further utilizes a cross-modal projector to map the graph embedding space to the input space of the language model. In this way, these studies reduce the reliance on task-specific labels.

However, these approaches primarily focus on the overall structure of the molecule level, failing to capture fine-grained knowledge of the sub-molecule level, such as functional groups. A natural tool to model sub-molecular structures is the motif [55], which refers to frequently recurring, significant subgraphs within molecular graphs. Motifs often play a key role in determining the properties of the whole molecular graph [55], and motif-level knowledge is frequently depicted in textual descriptions. As shown in Figure 1(b), a benzene ring indicating aromaticity property is reflected by the mention of "aromatic", and a carboxyl group is reflected by its name "carboxyl" in the description, revealing a fine-grained matching between motifs and texts.

Modeling the fine-grained motif-level knowledge is crucial for two reasons. First, motif-level knowledge is necessary for the generalization to unseen molecules, which are still largely composed of various motifs that have been seen before. For example, consider the zero-shot graph-text retrieval task shown in Figure 1(c), which aims to find the molecule most relevant to the given text. Even if the model has not been trained on the candidate molecules, it has seen many of the motifs within the unseen molecules such as the benzene and the ethyl group, corresponding to the words "benzene" and "carboxylic", respectively. Thus, the model can easily recognize the relevant molecule. Second, it bridges the gap for downstream tasks that require fine-grained knowledge. For example, in the molecule editing task illustrated in Figure 1(c), the model aims to modify part of the molecular structure based on textual instruction. This requires the model to understand the names or properties of the motifs like "chloride".

Despite the significance of this fine-grained knowledge, it is challenging to jointly learn both molecule- and motif-level knowledge, and also non-trivial to capture fine-grained matching without supervised signals. To overcome these issues, in this work, we propose a novel **Fine-grained Molecular graph-Text** framework (**FineMolTex**) to learn fine-grained motif-level knowledge, as well as coarse-grained molecule-level knowledge. First, we extract each motif or word token with an individual embedding for fine-grained knowledge and utilize two global tokens to holistically represent a molecular graph and its corresponding text description as coarse-grained knowledge. Second, to align coarse- and fine-grained matching, we propose two pre-training tasks respectively: the contrastive alignment task based on the global tokens, and the masked multi-modal learning task based on the motif and word tokens. Specifically, in the masked multi-modal modeling task illustrated in Figure 1(b), we randomly mask some motif and word tokens, and further incorporate a cross-attention transformer layer to integrate the embeddings of motifs and words. By predicting the labels of masked motifs and words based on information from each other, the learning of fine-grained alignment knowledge is enhanced. In summary, we outline our contributions as follows:

- We are the first to reveal that learning fine-grained motif-level knowledge provides key insight for bridging molecular graphs and text descriptions, further empowering the ability to generalize to unseen molecules and tasks.
- We introduce a novel framework named FineMolTex, consisting of two self-supervised pre-training tasks, to simultaneously learn coarse- and fine-grained knowledge. In particular, the masked

multi-modal learning task enhances the prediction for masked tokens leveraging information from the other modality, promoting the learning of fine-grained alignment information.

- Experimental results across three downstream tasks underscore the effectiveness of FineMolTex, with a notable improvement of up to 230% in the text-based molecule editing task. Furthermore, case studies demonstrate that FineMolTex effectively aligns motifs and words, further facilitating applications such as drug discovery and catalyst design.

2 Related Work

We provide a brief review on molecular multi-modal learning. Prior works predominantly concentrate on modeling the chemical structures such as 1D SMILES [17], 2D molecular graphs [7, 24, 55], and 3D geometric structures [38, 1, 41]. They utilize supervised signals on a predetermined set, and thus cannot generalize to unseen categories without labeled examples. Recently, KV-PLM [53] bridges this gap by linking SMILES with biomedical texts through a unified language modeling framework. Nonetheless, 1D SMILES may omit certain structural details and fail to identify structural similarities among molecules due to its non-uniqueness. To address these limitations, MoleculeSTM [26] and MoMu [35] employ a contrastive learning approach to align the molecular graph with its corresponding text, thus performing well on unseen molecules and texts. However, these models are less effective on molecule-to-text generation tasks because language models are not yet well-versed in interpreting graphs as generative conditions. Therefore, MolCA [27] introduces a cross-modal projector to align the embedding space of the molecular graph with the language model’s input space, enabling the comprehension of 2D graphs as generative conditions. This approach has also been extended to 3D graph structures, where 3D-MoLM [22] uses a cross-modal projector to synchronize the embedding space of the 3D geometric structure with that of the language model. Additionally, various efforts have been devoted to tackling specific molecular tasks based on textual data, including zero-shot instruction molecular learning [56], molecular reaction prediction [34], and molecular relational modeling [9].

More related works on graph-based molecular learning, as well as more general multi-modal learning, can be found in Appendix A.

3 The Proposed Approach

We propose FineMolTex, a novel fine-grained molecular graph-text framework, learning both molecule- and motif-level knowledge. The model architecture is outlined in Figure 2. This section first introduces the key components in the architecture, and then describes the two pre-training tasks.

3.1 Key Components of FineMolTex

To capture coarse- and fine-grained knowledge, we propose FineMolTex, consisting of five key components: 1) the tokenization component to decompose molecular graphs and texts into motif and word tokens; 2) a graph encoder to capture the structure of molecules and motifs; 3) a text encoder to extract the knowledge from texts and words; 4) a cross-attention layer to integrate information from different modalities; 5) a Transformer layer to generate embeddings for each token based on its contextual tokens from the same modality.

Tokenization. As shown in Figure 2, for fine-grained modeling, we fragment the molecular graphs and texts into motif tokens and word tokens. We employ the BRICS [6] algorithm to decompose molecular graphs into chemically significant motifs, followed by a post-processing procedure [55] to consolidate the motif vocabulary. We break the textual description into word tokens following SciBERT [3]. For coarse-grained modeling, the global tokens of molecule and text, <MOL> and <CLS>, are inserted at the beginning of the motif and word sequences, respectively, resulting in the sequences m_0, m_1, \dots, m_J and t_0, t_1, \dots, t_D , where J and D are the lengths of the sequences.

Graph Encoder. We utilize GraphMVP [25], a pre-trained Graph Isomorphism Network (GIN), to obtain the embedding of each motif token. It employs multi-view pre-training to connect the 2D topologies and 3D geometries in the GEOM dataset [2] containing 250K conformations. Let $\mathcal{G} = (\mathcal{V}, \mathcal{E}, \mathbf{X})$ denote a motif with N atoms, where $\mathcal{V} = \{v_1, v_2, \dots, v_N\}$ is the atom set, $\mathcal{E} \subseteq \mathcal{V} \times \mathcal{V}$ is the bond set, and $\mathbf{X} = [\mathbf{x}_1, \mathbf{x}_2, \dots, \mathbf{x}_N] \in \mathbb{R}^{N \times \zeta}$ represents the atom feature matrix, where \mathbf{x}_i is

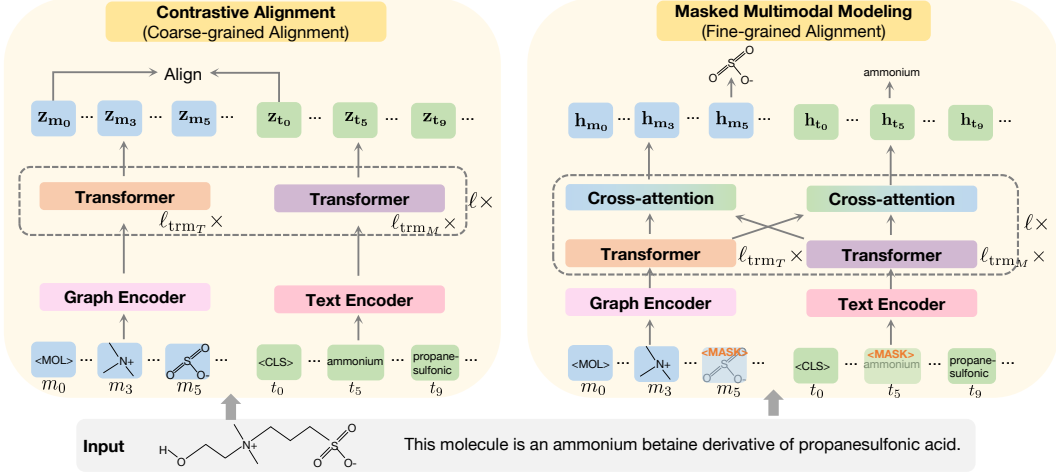


Figure 2: Architecture of FineMolTex. The input is a graph-text pair with both a molecular structure and a corresponding description. The components in the same color share the same weights.

the feature vector of atom v_i and ζ is the dimension of atom features. The embedding of each atom in the l -th layer is formed as

$$\mathbf{g}_v^{(l)} = \text{COMBINE}^{(l)} \left(\mathbf{g}_v^{(l-1)}, \text{AGGREGATE}^{(l)} \left(\{ \mathbf{g}_u^{(l-1)} : u \in \mathcal{N}(v) \} \right) \right), \quad (1)$$

where $\mathbf{g}_v^{(l)}$ is the embedding of atom v at l -th layer, $\mathcal{N}(v)$ is the neighbors of atom v , AGGREGATE(\cdot) aggregates the neighborhood information of atom v , and COMBINE(\cdot) further combines the self-information with the neighborhood information. Then, we pool the atom embeddings at the final layer ℓ_g into a motif-level embedding, \mathbf{g}_G , as follows.

$$\mathbf{g}_G = \text{READOUT}(\{ \mathbf{g}_v^{(\ell_g)} | v \in G \}), \quad \text{for } G \in \{m_1, m_2, \dots, m_J\}, \quad (2)$$

where READOUT(\cdot) is permutation invariant, implemented as the average function in our model.

Text Encoder. We use SciBERT [3], which has been pre-trained on texts from the chemical and biological domains, as our text encoder, denoted as f_{bert} . It can encode a text sequence as:

$$\mathbf{b}_{t_0}, \mathbf{b}_{t_1}, \dots, \mathbf{b}_{t_D} = f_{\text{bert}}(t_0, t_1, \dots, t_D). \quad (3)$$

Transformer Layer. To capture the contextual information for each token, we use “encoder-style” Transformer layers [39], which consist of a multi-head self-attention layer and a fully connected feed-forward network. This enables the tokens to gather information from other tokens in the same modality. We utilize f_{trm_T} and f_{trm_M} for the text and molecule modality, respectively, as follows.

$$\mathbf{z}_{t_0}, \mathbf{z}_{t_1}, \dots, \mathbf{z}_{t_D} = f_{\text{trm}_T}(\mathbf{b}_{t_0}, \mathbf{b}_{t_1}, \dots, \mathbf{b}_{t_D}), \quad (4)$$

$$\mathbf{z}_{m_0}, \mathbf{z}_{m_1}, \dots, \mathbf{z}_{m_J} = f_{\text{trm}_M}(\mathbf{g}_{m_0}, \mathbf{g}_{m_1}, \dots, \mathbf{g}_{m_J}). \quad (5)$$

Cross-attention Layer. We integrate information from different modalities via cross-attention layers f_{crs_M} and f_{crs_T} for molecular graph and text, respectively. Consider the cross-attention layer f_{crs_M} for molecular graph: the queries are from the same modality, $Q_m = Z_m W_m^Q$, while the keys and values are from the text modality, $K_t = Z_t W_t^K$ and $V_t = Z_t W_t^V$. Here W_m^Q , W_t^K , W_t^V are learnable weights, $Z_m = [\mathbf{z}_{m_0}, \mathbf{z}_{m_1}, \dots, \mathbf{z}_{m_J}]$, and $Z_t = [\mathbf{z}_{t_0}, \mathbf{z}_{t_1}, \dots, \mathbf{z}_{t_K}]$. Subsequently, the output of scaled dot-product attention is computed as:

$$\text{Attention}(Q_m, K_t, V_t) = \text{softmax} \left(\frac{Q_m K_t^T}{\sqrt{d_k}} \right) V_t, \quad (6)$$

where d_k is the dimension of queries and keys. The cross-attention layer for text is designed similarly. Hence, the encoding of each token accounts for tokens from the other modality, enabling the learning of fine-grained alignment at the motif level. The outputs of the cross-attention layer are:

$$\mathbf{h}_{t_0}, \mathbf{h}_{t_1}, \dots, \mathbf{h}_{t_D} = f_{\text{crs}_T}(\mathbf{z}_{t_0}, \mathbf{z}_{t_1}, \dots, \mathbf{z}_{t_D}), \quad (7)$$

$$\mathbf{h}_{m_0}, \mathbf{h}_{m_1}, \dots, \mathbf{h}_{m_J} = f_{\text{crs}_M}(\mathbf{z}_{m_0}, \mathbf{z}_{m_1}, \dots, \mathbf{z}_{m_J}). \quad (8)$$

3.2 Pre-training Tasks

We propose two pre-training tasks, the contrastive alignment task for coarse-grained alignment, and the masked multi-modal modeling task for fine-grained alignment.

Contrastive Alignment. For coarse-grained alignment at the molecule level, we align the graph-text pairs from the same molecules and contrast the pairs from different molecules, which can be achieved by optimizing the following loss.

$$L_{\text{con}} = -\frac{1}{2}\mathbb{E}_{m_0, t_0} \left[\log \frac{\exp(\cos(\mathbf{z}_{m_0}, \mathbf{z}_{t_0})/\tau)}{\exp(\cos(\mathbf{z}_{m_0}, \mathbf{z}_{t_0})/\tau) + \sum_{t'_0} \exp(\cos(\mathbf{z}_{m_0}, \mathbf{z}_{t'_0})/\tau)} + \log \frac{\exp(\cos(\mathbf{z}_{t_0}, \mathbf{z}_{m_0})/\tau)}{\exp(\cos(\mathbf{z}_{t_0}, \mathbf{z}_{m_0})/\tau) + \sum_{m'_0} \exp(\cos(\mathbf{z}_{t_0}, \mathbf{z}_{m'_0})/\tau)} \right], \quad (9)$$

where \mathbf{z}_{m_0} , $\mathbf{z}_{m'_0}$, \mathbf{z}_{t_0} , and $\mathbf{z}_{t'_0}$ denote the output embeddings from the Transformer layer, t'_0 and m'_0 are the negative instances sampled from the same batch of graph-text pairs, and $\cos(\cdot, \cdot)/\tau$ is the cosine similarity scaled by the temperature hyperparameter τ . In this way, we capture the molecule-level knowledge, aligning the embedding space of molecular graphs and texts holistically.

Masked Multi-modal Modeling. For fine-grained alignment at the motif level, we mask some of the tokens and predict their labels. Based on the fragmented motifs of all molecules in the pre-training dataset, we construct a motif dictionary that includes motifs along with their labels and frequency. Then we randomly mask approximately 20% of the motif tokens that have neither too high nor too low a frequency in the motif dictionary, as well as 15% of the word tokens. The token embeddings of the motifs and words are updated utilizing ℓ_{trm_M} and ℓ_{trm_T} transformer layers, respectively. Subsequently, information from the two modalities is integrated via our cross-attention layer. This entire process is iterated for ℓ times.

Based on the output embeddings of fine-grained tokens from the cross-attention layer $\mathbf{h}_{t_1}, \dots, \mathbf{h}_{t_D}$ and $\mathbf{h}_{m_0}, \mathbf{h}_{m_1}, \dots, \mathbf{h}_{m_J}$, we utilize two classifiers ρ_m and ρ_t to predict the labels of the masked motifs and words: $\hat{y}_{m_i} = \rho_m(\mathbf{h}_{m_i})$, $\hat{y}_{t_j} = \rho_t(\mathbf{h}_{t_j})$, where \hat{y}_{m_i} is the predicted label of motif m_i , and \hat{y}_{t_j} is the predicted label of word t_j . Given the ground truth labels y_{m_i} and y_{t_j} , the model is trained by reconstructing the masked tokens as:

$$L_{\text{pre}} = \beta \sum_i \text{CE}(\hat{y}_{m_i}, y_{m_i}) + \alpha \sum_j \text{CE}(\hat{y}_{t_j}, y_{t_j}), \quad (10)$$

where α, β are hyperparameters, and $\text{CE}(\cdot, \cdot)$ is the cross-entropy loss. The key to achieving fine-grained alignment lies in the cross-attention layer, which enables the model to predict the labels of masked tokens based on tokens from the other modality. For instance, as illustrated in Figure 2, predicting the label of SO_3^- solely based on the unmasked motif tokens is challenging. However, by leveraging the embeddings of word tokens, particularly "propanesulfonic" which includes the SO_3^- group, we can gain relevant information about the masked token. Consequently, the model implicitly learns fine-grained alignment knowledge, thereby augmenting its motif-level knowledge.

Overall Loss. FinMolTex is optimized by the overall loss $L = L_{\text{con}} + L_{\text{pre}}$. Thus, FineMolTex is able to jointly learn the molecule- and motif-level knowledge.

4 Experiments

In this section, we conduct extensive experiments to demonstrate the effectiveness of FineMolTex. Before evaluating, we first conduct the two pre-training tasks on the PubChemSTM dataset [26], which includes 281K graph-text pairs from PubChem [16]. Each molecular graph is paired with a textual description that elaborates on its chemical and physical properties or highlights its high-level bioactivities. Details of the pre-training data and process can be found in Appendix C.1.1 and C.4.

The goal of our experiments is to answer the following research questions (RQs).

RQ1. Can FineMolTex better generalize to unseen molecules?

RQ2. Can FineMolTex bridge the gap to tasks centered on motif-level knowledge?

RQ3. Can FineMolTex perform better on single-modality tasks?

Table 1: Accuracy ($\% \pm \sigma$) of graph-text retrieval task on DrugBank-Pharmacodynamics.

T	Given Molecular Graph			Given Text		
	4	10	20	4	10	20
KV-PLM	68.38 \pm 0.03	47.59 \pm 0.03	36.54 \pm 0.03	67.68 \pm 0.03	48.00 \pm 0.02	34.66 \pm 0.02
MolCA	83.75 \pm 0.54	74.25 \pm 0.26	66.14 \pm 0.21	81.27 \pm 0.33	69.46 \pm 0.17	62.13 \pm 0.16
MoMu-S	70.51 \pm 0.04	55.20 \pm 0.15	43.78 \pm 0.10	70.71 \pm 0.22	54.70 \pm 0.31	44.25 \pm 0.43
MoMu-K	69.40 \pm 0.11	53.14 \pm 0.26	42.32 \pm 0.28	68.71 \pm 0.03	53.29 \pm 0.05	43.83 \pm 0.12
MoleculeSTM	92.14 \pm 0.02	86.27 \pm 0.02	81.08 \pm 0.05	91.44 \pm 0.02	86.76 \pm 0.03	81.68 \pm 0.03
FineMolTex	95.86\pm0.34	91.95\pm0.06	85.80\pm0.05	95.80\pm0.06	92.18\pm0.12	85.01\pm0.32

Table 2: Accuracy ($\% \pm \sigma$) of graph-text retrieval task on molecule-ATC.

T	Given Molecular Graph			Given Text		
	4	10	20	4	10	20
KV-PLM	60.94 \pm 0.00	42.35 \pm 0.00	30.32 \pm 0.00	60.67 \pm 0.00	40.19 \pm 0.00	29.02 \pm 0.00
MolCA	67.34 \pm 0.05	53.51 \pm 0.12	44.10 \pm 0.03	65.18 \pm 0.34	51.01 \pm 0.26	41.30 \pm 0.51
MoMu-S	64.72 \pm 0.04	48.72 \pm 0.03	37.64 \pm 0.02	64.98 \pm 0.13	49.58 \pm 0.05	39.04 \pm 0.16
MoMu-K	61.79 \pm 0.14	45.69 \pm 0.22	34.55 \pm 0.09	63.32 \pm 0.15	47.55 \pm 0.06	37.68 \pm 0.18
MoleculeSTM	69.33 \pm 0.03	54.83 \pm 0.04	44.13 \pm 0.05	71.81 \pm 0.05	58.34 \pm 0.07	47.58 \pm 0.05
FineMolTex	75.43\pm0.15	60.66\pm0.08	49.45\pm0.24	75.22\pm0.12	60.29\pm0.04	48.42\pm0.15

RQ4. Has FineMolTex learned fine-grained knowledge?

RQ5. Are the token masking and cross-attention layers beneficial?

4.1 Generalization to Unseen Molecules (RQ1)

To answer RQ1, we conduct a **zero-shot graph-text retrieval task** to examine the generalizability of FineMolTex on unseen molecules and texts. Given a molecular graph and T candidate textual descriptions, the goal is to identify the textual description that best aligns with the molecular graph. Conversely, given a textual description and T candidate molecular graphs, identify the molecular graph that best matches the text. This task can be addressed by calculating the similarity of the molecular graphs and texts in the joint embedding space, thus allowing zero-shot inference.

Datasets and Baselines. We utilize DrugBank-Pharmacodynamics, molecule-ATC, and DrugBank-Description [26] extracted from the DrugBank database [44] for evaluation. These datasets include molecular graphs and their chemical descriptions. Details of the datasets can be found in Appendix C.1.2. We compare with five multimodal molecular models: KV-PLM [53], MolCA [27], MoMu-S [35], MoMu-K [35], and MoleculeSTM [26]. Specifically, KV-PLM uses SMILES to represent the structure of the molecule, while others use graph structures.

Results. We report the results on the first two datasets in Tables 1 and 2, and defer those on DrugBank-Description to Appendix D.1 due to space limit. We make the following observations. 1) Across different values of T , FineMolTex consistently outperforms the baselines that neglect motif-level knowledge. The superior performance demonstrates that fine-grained motif-level knowledge facilitates generalization to unseen molecules, which likely contain seen motifs. 2) FineMolTex maintains strong performance in both directions (given graph, and given text). The symmetry further indicates that the embedding spaces of both modalities are well-aligned and similarly well-learned. 3) We observe that KV-PLM, which utilizes SMILES to capture molecular structures, is less effective than other models employing graphs, consistent with previous findings [26] that 2D graph structure is more expressive than 1D SMILES.

4.2 Application to Motif-Centered Tasks (RQ2)

To answer RQ2, we employ a zero-shot **text-based molecule editing task**, which is highly relevant to practical applications including catalyst design and targeted drug discovery. Specifically, we utilize FineMolTex to collaborate with a molecule generation module, following the design in [26], to modify a specified molecule according to a text prompt. Hence, motif-level knowledge is essential for this task, as the model needs to replace certain motifs with others that are related to specific properties and names as indicated in the text prompt. We defer the technical details to Appendix B. We randomly sample 200 molecules from ZINC [14], and select 12 text prompts, including 8 prompts pertaining to physical properties [26], and 4 based on the names of the motifs. We utilize MoleculeSTM, MoMu, and MolCA as baselines.

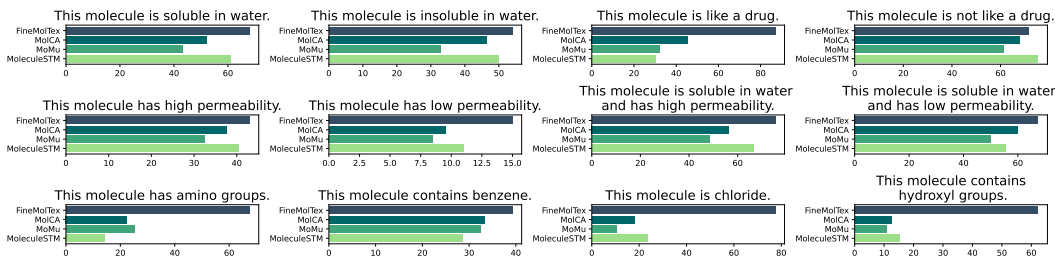


Figure 3: Hit ratios of 12 text-based molecule editing tasks.

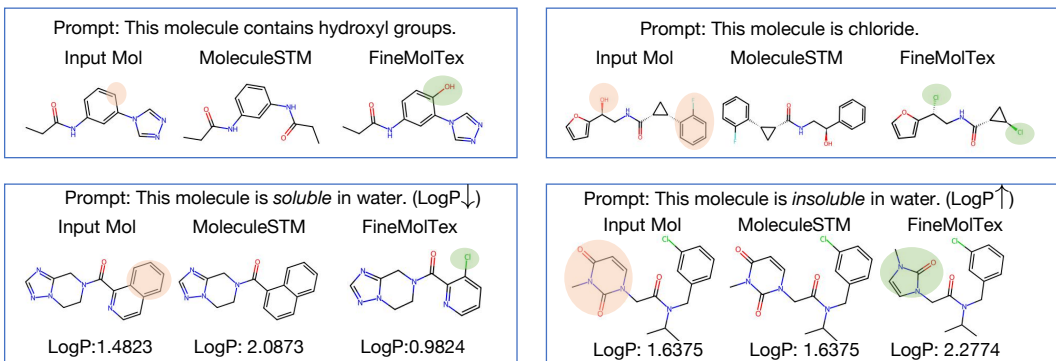


Figure 4: Visual analysis of the output molecules of MoleculeSTM and Motif-MolTex on 4 text-based molecule editing tasks. Differences between the input and output molecule of FineMolTex are highlighted in red and green circles. Lower LogP indicates higher water solubility.

Evaluation. We employ different methods to assess whether the generated molecules satisfy the two types of prompts. For the 8 prompts on physical properties, we employ three measures: LogP, QED, and tPSA, which measures solubility [21], drug-likeness [4], and permeability [8], respectively. We consider the editing to be successful if the difference in measurements between the input and output molecules exceeds a specified threshold Δ , which we have set to 0 following one of the settings in literature [26]. For the 4 prompts based on motif names, we use RDKit [20] to verify the presence of the indicated motifs. For all 12 prompts, we report the *hit ratio*: the proportion of generated molecules that meet our expectations.

Results. As shown in Figure 3, FineMolTex shows superior performance on these prompts, especially on the 4 prompts with motif names. Notably, we achieve a relative gain of up to 230% over the best-performing baseline, demonstrating that FineMolTex has an advanced understanding of motif-level knowledge. We also visualize the output molecules of MoleculeSTM and FineMolTex in Figure 4. It can be observed that while MoleculeSTM produces incorrect molecules, FineMolTex accurately generates the intended molecules. Specifically, when prompted to generate molecules that are soluble in water, FineMolTex successfully creates molecules with lower LogP than the input molecule, as lower LogP indicates higher water solubility. Similarly, when prompted to generate molecules with hydroxyl groups or chlorine atoms, FineMolTex correctly does so. These results confirm that FineMolTex possesses a deeper understanding of motif-level knowledge, thereby enhancing the generative capabilities. More visual results can be seen in Appendix D.2.

4.3 Application to Single-Modality Task (RQ3)

While FineMolTex can simultaneously utilize pre-trained knowledge from both graphs and texts, we also verify its effectiveness on single-modality tasks, namely, **molecular property prediction tasks**. We use MoleculeNet [46] as the dataset, which only provides molecular graphs as input without texts. More specifically, there are eight binary classification tasks, and we report ROC-AUC for evaluation. More detailed dataset descriptions are provided in Appendix C.1.3.

Baselines. We compare FineMolTex against nine baselines, including 1) five pre-trained GNN models: AttrMasking [12], ContextPred [12], InfoGraph [36], MolCLR [43], and GraphMVP [25];

Table 3: Downstream results ($\% \pm \sigma$) on eight binary classification datasets from MoleculeNet.

Model	BBBP	Tox21	ToxCast	Sider	ClinTox	MUV	HIV	Bace	Avg
AttrMask	67.8 \pm 2.6	75.0 \pm 0.2	63.6 \pm 0.8	58.1 \pm 1.2	75.4 \pm 8.8	73.8 \pm 1.2	75.4 \pm 0.5	80.3 \pm 0.0	71.2
ContextPred	63.1 \pm 3.5	74.3 \pm 0.2	61.6 \pm 0.5	60.3 \pm 0.8	80.3 \pm 3.8	71.4 \pm 1.4	70.7 \pm 3.6	78.8 \pm 0.4	70.1
InfoGraph	64.8 \pm 0.6	76.2 \pm 0.4	62.7 \pm 0.7	59.1 \pm 0.6	76.5 \pm 7.8	73.0 \pm 3.6	70.2 \pm 2.4	77.6 \pm 2.0	70.0
MolCLR	67.8 \pm 0.5	67.8 \pm 0.5	64.6 \pm 0.1	58.7 \pm 0.1	84.2 \pm 1.5	72.8 \pm 0.7	75.9 \pm 0.2	71.1 \pm 1.2	71.3
GraphMVP	68.1 \pm 1.4	77.1 \pm 0.4	65.1 \pm 0.3	60.6 \pm 0.1	84.7 \pm 3.1	74.4 \pm 2.0	77.7 \pm 2.5	80.5 \pm 2.7	73.5
GraphCL	69.7 \pm 0.7	73.9 \pm 0.7	62.4 \pm 0.6	60.5 \pm 0.9	76.0 \pm 2.7	69.8 \pm 2.7	78.5 \pm 1.2	75.4 \pm 1.4	70.8
KV-PLM	70.5 \pm 0.5	72.1 \pm 1.0	55.0 \pm 1.7	59.8 \pm 0.6	89.2 \pm 2.7	54.6 \pm 4.8	65.4 \pm 1.7	78.5 \pm 2.7	68.2
MoMu-S	70.5 \pm 2.0	75.6 \pm 0.3	75.6 \pm 0.3	60.5 \pm 0.9	79.9 \pm 4.1	70.5 \pm 1.4	75.9 \pm 0.8	76.7 \pm 2.1	71.6
MoMu-K	70.1 \pm 1.4	75.6 \pm 0.5	63.0 \pm 0.4	60.4 \pm 0.8	77.4 \pm 4.1	71.1 \pm 2.7	76.2 \pm 0.9	77.1 \pm 1.4	71.4
MolCA	70.0 \pm 0.5	77.2 \pm 0.5	64.5 \pm 0.8	63.0 \pm 1.7	89.5 \pm 0.7	72.1 \pm 1.3	77.2 \pm 0.6	79.8 \pm 0.5	74.2
MoleculeSTM	70.0 \pm 0.5	76.9 \pm 0.5	65.1 \pm 0.4	61.0 \pm 1.05	92.5 \pm 1.1	73.4 \pm 2.9	77.0 \pm 1.8	80.8 \pm 1.3	74.6
FineMolTex	71.0\pm0.4	77.1\pm0.5	66.0\pm1.2	65.0\pm2.3	92.7\pm0.8	76.2\pm1.2	78.9\pm0.6	84.6\pm1.4	76.4

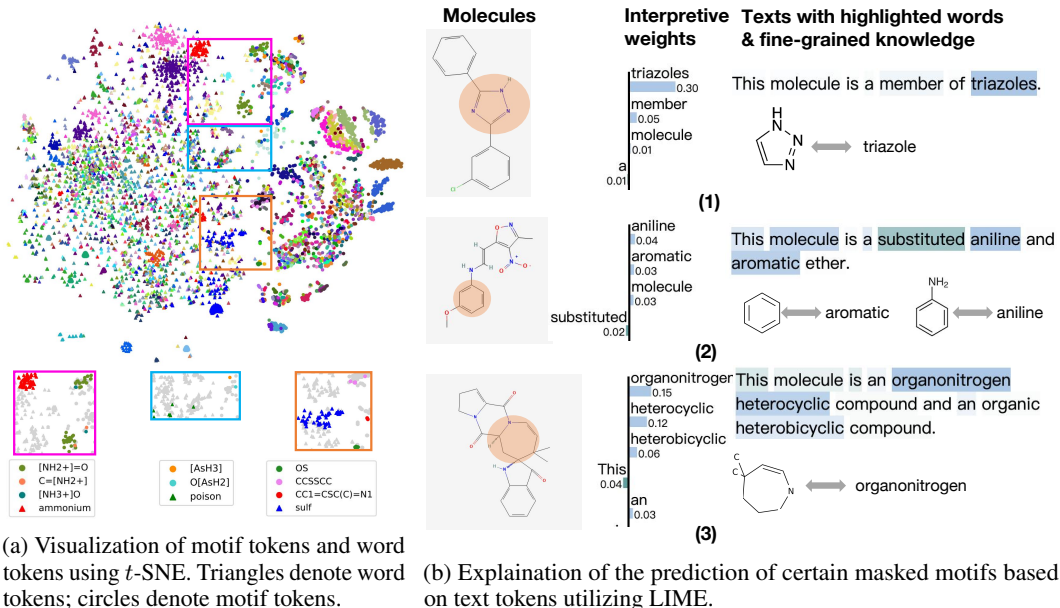


Figure 5: Case studies validating motif-level knowledge learned by our model.

2) three graph-text multimodal models: MoMu-S [35], MoMu-K [35], and MoleculeSTM [26], and
 3) one SMILES-text multimodal model: KV-PLM [53].

Results. As shown in Table 3, FineMolTex consistently outperforms all baselines, achieving relative gains of 3.2%, 2.4%, and 4.7% on SIDER, MUV, and BACE, respectively, compared to the best baseline. The promising performance of FineMolTex indicates that it implicitly utilizes pre-trained knowledge from the text modality even when the input consists solely of graphs. Additionally, KV-PLM exhibits a notable performance gap from other models, due to its use of 1D SMILES strings for molecular structure and a smaller pre-training dataset.

4.4 Analysis of Learned Fine-grained Knowledge (RQ4)

We evaluate whether FineMolTex captures fine-grained alignment information in the joint embedding space, and assess if it can predict the labels of masked motifs based on fine-grained knowledge.

Visualization of Motif and Word Embeddings. To evaluate whether FineMolTex captures fine-grained alignment knowledge, we select motif and word tokens from 1,500 graph-text pairs in the PubChemSTM dataset, excluding meaningless words such as “this” and “a”. In total, we visualize 3,469 motif tokens and 6,914 text tokens with *t*-SNE [29] in Figure 5a, where triangles denote text tokens, and circles denote motif tokens, with different colors indicating various labels. To examine the details of the tokens, we zoom into several regions in the figure, retaining only the colors and legends of the tokens we are interested in. For brevity, we utilize SMILES to represent the motif structures. We observe that text and motif tokens corresponding to each other are also close in the embedding space. For instance, in the orange frame, the word “sulf” is close to the motif tokens

Table 4: Ablation study ($\% \pm \sigma$) on molecule-ATC and DrugBank-Pharmacodynamics.

	molecule-ATC		DrugBank-Pharmacodynamics	
	Given Molecular Graph	Given Text	Given Molecular Graph	Given Text
FineMolTex w/o mmm	70.33 \pm 0.28	70.86 \pm 0.16	92.56 \pm 0.10	92.12 \pm 0.25
FineMolTex w/o mask word	72.85 \pm 0.46	71.15 \pm 0.24	93.45 \pm 0.44	92.98 \pm 0.18
FineMolTex w/o mask motif	74.27 \pm 0.07	72.11 \pm 0.13	94.86 \pm 0.32	93.88 \pm 0.15
FineMolTex w/o cross	71.44 \pm 0.32	70.92 \pm 0.18	92.66 \pm 0.08	92.85 \pm 0.24
FineMolTex	75.43\pm0.15	75.22\pm0.12	95.86\pm0.34	95.80\pm0.06

“OS”, “CCSSCC”, and “CC1=CSC(C)=N1”, all of which represent sulfides. In the pink frame, the word “ammonium” is close to the motif tokens “[NH2+]=O”, “C=[NH2+]”, and “[NH3+]O”, which are related to “ammonium.” In the blue frame, the word “poison” is adjacent to the motifs “[AsH3]” and “[O[AsH2]”, which are poisonous. These results demonstrate that FineMolTex learns the connections between motifs and their chemical names and properties, thereby significantly enhancing its expressiveness.

Predictions Based on Fine-grained knowledge. To further verify that FineMolTex can utilize the learned fine-grained alignment knowledge for predictions, we utilize Local Interpretable Model-Agnostic Explanation (LIME) [31], a well-established tool that can explain the predictions of certain masked motifs based on text tokens. By perturbing the input text, LIME observes how the model’s predictions change with variations in the input text. Then, LIME fits these perturbed texts and the prediction results to an interpretable model such as a linear model. This approach allows us to quantify the significance of each text token in predicting the motifs, thereby revealing the fine-grained knowledge learned by FineMolTex. The results are shown in Figure 5b (with more cases in Appendix D.4), where text tokens with higher interpretive weights are more crucial for predictions, and thus more relevant to the masked motifs. Specifically, the word with the highest interpretive weights in (1) is “triazoles”, which directly is to the name of the masked motif. In (2), the word “aniline” refers to another motif that is very similar to the masked motif, and “aromatic” is the property related to the masked motif. In (3), the masked motif is a kind of “organonitrogen”. These findings demonstrate that FineMolTex has effectively acquired motif-level knowledge.

4.5 Ablation Study for Masking and Cross-Attention Layers (RQ5)

To thoroughly explore the impact of the key components in FineMolTex, we compare to several variants, including **FineMolTex w/o mmm**, which drops the masked multimodal modeling task altogether; **FineMolTex w/o mask word**, which does not mask word tokens; **FineMolTex w/o mask motif**, which does not mask motif tokens; **FineMolTex w/o cross**, which excludes cross-attention layers. We evaluate these variants on the graph-text retrieval task used in RQ1, on two datasets with $T = 4$. As reported in Table 4, our model consistently surpasses the other variants. Specifically, without the masked multimodal modeling task, “FineMolTex w/o mmm” fails to capture fine-grained knowledge, resulting in the poorest performance. While “FineMolTex w/o mask word” and “FineMolTex w/o mask motif” perform better than “FineMolTex w/o mmm,” they are less effective than FineMolTex, which masks both words and motifs for mutual alignment. Lastly, without the cross-attention layers, “FineMolTex w/o cross” cannot integrate token embeddings from different modalities, thereby hampering its ability to effectively learn fine-grained knowledge. These observations demonstrate the effectiveness of each component.

5 Conclusions, Limitations and Broader Impact

In this paper, we reveal that fine-grained motif-level knowledge is crucial for molecular representation learning. We propose FineMolTex to jointly learn both coarse- and fine-grained knowledge through a contrastive alignment task and a masked multimodal learning task, respectively. By masking the fine-grained tokens and predicting their labels using tokens from the other modality, we can effectively learn fine-grained alignment between motifs and words. Experimental results on three downstream tasks and two case studies demonstrate the effectiveness of FineMolTex.

Limitations. Despite the promising results of FineMolTex, the molecular graph-text dataset is small in scale, hindering the cross-modal understanding. To overcome the limitation, we plan to seek more

high-quality texts closely related to molecular graphs or devise an approach to align the embedding spaces of molecular graphs and texts without paired data.

Broader Impact. We demonstrate the importance of capturing fine-grained motif-level knowledge through diverse downstream tasks. Consequently, our research has the potential to contribute to the development of a foundation model for various chemical and biomedical applications, paving a promising way for key scientific inquiries, including drug discovery, molecular reaction prediction, and molecular property prediction.

References

- [1] Kenneth Atz, Francesca Grisoni, and Gisbert Schneider. Geometric deep learning on molecular representations. *Nat. Mach. Intell.*, 3(12):1023–1032, 2021.
- [2] Simon Axelrod and Rafael Gómez-Bombarelli. Geom, energy-annotated molecular conformations for property prediction and molecular generation. *Scientific Data*, Apr 2022.
- [3] Iz Beltagy, Kyle Lo, and Arman Cohan. Scibert: A pretrained language model for scientific text. *arXiv preprint arXiv:1903.10676*, 2019.
- [4] G. Richard Bickerton, Gaia V. Paolini, Jérémy Besnard, Sorel Muresan, and Andrew L. Hopkins. Quantifying the chemical beauty of drugs. *Nature Chemistry*, page 90–98, Feb 2012.
- [5] Tox21 Data Challenge. Tox21 data challenge 2014. <https://tripod.nih.gov/tox21/challenge/>, 2014. Accessed: 2024-05-20.
- [6] Jörg Degen, Christof Wegscheid-Gerlach, Andrea Zaliani, and Matthias Rarey. On the art of compiling and using “drug-like” chemical fragment spaces. *ChemMedChem*, page 1503–1507, Oct 2008.
- [7] David Duvenaud, Dougal Maclaurin, Jorge Aguilera-Iparraguirre, Rafael Gómez-Bombarelli, Timothy Hirzel, Alán Aspuru-Guzik, and Ryan P. Adams. Convolutional networks on graphs for learning molecular fingerprints. In Corinna Cortes, Neil D. Lawrence, Daniel D. Lee, Masashi Sugiyama, and Roman Garnett, editors, *Advances in Neural Information Processing Systems 28: Annual Conference on Neural Information Processing Systems 2015, December 7-12, 2015, Montreal, Quebec, Canada*, pages 2224–2232, 2015.
- [8] Peter Ertl, Bernhard Rohde, and Paul Selzer. Fast calculation of molecular polar surface area as a sum of fragment-based contributions and its application to the prediction of drug transport properties. *Journal of Medicinal Chemistry*, 43(20):3714–3717, Oct 2000.
- [9] Junfeng Fang, Shuai Zhang, Chang Wu, Zhengyi Yang, Zhiyuan Liu, Sihang Li, Kun Wang, Wenjie Du, and Xiang Wang. Moltc: Towards molecular relational modeling in language models. *CoRR*, abs/2402.03781, 2024.
- [10] Kaitlyn M Gayvert, Neel S Madhukar, and Olivier Elemento. A data-driven approach to predicting successes and failures of clinical trials. *Cell chemical biology*, 23(10):1294–1301, 2016.
- [11] Justin Gilmer, Samuel S Schoenholz, Patrick F Riley, Oriol Vinyals, and George E Dahl. Neural message passing for quantum chemistry. In *International conference on machine learning*, pages 1263–1272. PMLR, 2017.
- [12] Weihua Hu, Bowen Liu, Joseph Gomes, Marinka Zitnik, Percy Liang, Vijay Pande, and Jure Leskovec. Strategies for pre-training graph neural networks. *arXiv preprint arXiv:1905.12265*, 2019.
- [13] Weihua Hu, Bowen Liu, Joseph Gomes, Marinka Zitnik, Percy Liang, Vijay S. Pande, and Jure Leskovec. Strategies for pre-training graph neural networks. In *8th International Conference on Learning Representations, ICLR 2020, Addis Ababa, Ethiopia, April 26-30, 2020*. OpenReview.net, 2020.

- [14] John J Irwin, Teague Sterling, Michael M Mysinger, Erin S Bolstad, and Ryan G Coleman. Zinc: a free tool to discover chemistry for biology. *Journal of chemical information and modeling*, 52(7):1757–1768, 2012.
- [15] Dahun Kim, Anelia Angelova, and Weicheng Kuo. Region-aware pretraining for open-vocabulary object detection with vision transformers.
- [16] Sunghwan Kim, Jie Chen, Tiejun Cheng, Asta Gindulyte, Jia He, Siqian He, Qingliang Li, Benjamin A Shoemaker, Paul A Thiessen, Bo Yu, et al. Pubchem in 2021: new data content and improved web interfaces. *Nucleic acids research*, 49(D1):D1388–D1395, 2021.
- [17] Mario Krenn, Florian Häse, AkshatKumar Nigam, Pascal Friederich, and Alán Aspuru-Guzik. Self-referencing embedded strings (SELFIES): A 100% robust molecular string representation. *Mach. Learn. Sci. Technol.*, 1(4):45024, 2020.
- [18] Michael Kuhn, Ivica Letunic, Lars Juhl Jensen, and Peer Bork. The sider database of drugs and side effects. *Nucleic acids research*, 44(D1):D1075–D1079, 2016.
- [19] Weicheng Kuo, Yin Cui, Xiuye Gu, AJ Piergiovanni, and Anelia Angelova. F-vlm: Open-vocabulary object detection upon frozen vision and language models. Sep 2022.
- [20] G Landrum. Rdkit: Open-source cheminformatics, 2024.
- [21] Leo Leo, Albert Albert, Hansch Hansch, Corwin Corwin, Elkins Elkins, and David David. Partition coefficients and their uses. Jan 1971.
- [22] Sihang Li, Zhiyuan Liu, Yanchen Luo, Xiang Wang, Xiangnan He, Kenji Kawaguchi, Tat-Seng Chua, and Qi Tian. Towards 3d molecule-text interpretation in language models. *CoRR*, abs/2401.13923, 2024.
- [23] Chuang Lin, Peize Sun, Yi Jiang, Ping Luo, Lizhen Qu, Gholamreza Haffari, Zehuan Yuan, and Jianfei Cai. Learning object-language alignments for open-vocabulary object detection. Nov 2022.
- [24] Shengchao Liu, Mehmet Furkan Demirel, and Yingyu Liang. N-gram graph: Simple unsupervised representation for graphs, with applications to molecules. In Hanna M. Wallach, Hugo Larochelle, Alina Beygelzimer, Florence d’Alché-Buc, Emily B. Fox, and Roman Garnett, editors, *Advances in Neural Information Processing Systems 32: Annual Conference on Neural Information Processing Systems 2019, NeurIPS 2019, December 8-14, 2019, Vancouver, BC, Canada*, pages 8464–8476, 2019.
- [25] Shengchao Liu, Mehmet Furkan Demirel, and Yingyu Liang. N-gram graph: Simple unsupervised representation for graphs, with applications to molecules. In Hanna M. Wallach, Hugo Larochelle, Alina Beygelzimer, Florence d’Alché-Buc, Emily B. Fox, and Roman Garnett, editors, *Advances in Neural Information Processing Systems 32: Annual Conference on Neural Information Processing Systems 2019, NeurIPS 2019, December 8-14, 2019, Vancouver, BC, Canada*, pages 8464–8476, 2019.
- [26] Shengchao Liu, Weili Nie, Chengpeng Wang, Jiarui Lu, Zhuoran Qiao, Ling Liu, Jian Tang, Chaowei Xiao, and Animashree Anandkumar. Multi-modal molecule structure–text model for text-based retrieval and editing. *Nature Machine Intelligence*, 5(12):1447–1457, 2023.
- [27] Zhiyuan Liu, Sihang Li, Yanchen Luo, Hao Fei, Yixin Cao, Kenji Kawaguchi, Xiang Wang, and Tat-Seng Chua. Molca: Molecular graph-language modeling with cross-modal projector and uni-modal adapter. In Houda Bouamor, Juan Pino, and Kalika Bali, editors, *Proceedings of the 2023 Conference on Empirical Methods in Natural Language Processing, EMNLP 2023, Singapore, December 6-10, 2023*, pages 15623–15638. Association for Computational Linguistics, 2023.
- [28] Chuofan Ma, Yi Jiang, Xin Wen, Zehuan Yuan, and Xiaojuan Qi. Codet: Co-occurrence guided region-word alignment for open-vocabulary object detection. *Advances in Neural Information Processing Systems*, 36, 2024.
- [29] Laurensvander Maaten and GeoffreyE. Hinton. Visualizing data using t-sne. *Journal of Machine Learning Research, Journal of Machine Learning Research*, Jan 2008.

- [30] Ines Filipa Martins, Ana L. Teixeira, Luis Pinheiro, and André O. Falcão. A bayesian approach to *in Silico* blood-brain barrier penetration modeling. *J. Chem. Inf. Model.*, 52(6):1686–1697, 2012.
- [31] Marco Túlio Ribeiro, Sameer Singh, and Carlos Guestrin. "why should I trust you?": Explaining the predictions of any classifier. In Balaji Krishnapuram, Mohak Shah, Alexander J. Smola, Charu C. Aggarwal, Dou Shen, and Rajeev Rastogi, editors, *Proceedings of the 22nd ACM SIGKDD International Conference on Knowledge Discovery and Data Mining, San Francisco, CA, USA, August 13-17, 2016*, pages 1135–1144. ACM, 2016.
- [32] Sebastian G Rohrer and Knut Baumann. Maximum unbiased validation (muv) data sets for virtual screening based on pubchem bioactivity data. *Journal of chemical information and modeling*, 49(2):169–184, 2009.
- [33] Yu Rong, Yatao Bian, Tingyang Xu, Weiyang Xie, Ying Wei, Wenbing Huang, and Junzhou Huang. Self-supervised graph transformer on large-scale molecular data. *Advances in neural information processing systems*, 33:12559–12571, 2020.
- [34] Yaorui Shi, An Zhang, Enzhi Zhang, Zhiyuan Liu, and Xiang Wang. Relm: Leveraging language models for enhanced chemical reaction prediction. In Houda Bouamor, Juan Pino, and Kalika Bali, editors, *Findings of the Association for Computational Linguistics: EMNLP 2023, Singapore, December 6-10, 2023*, pages 5506–5520. Association for Computational Linguistics, 2023.
- [35] Bing Su, Dazhao Du, Zhao Yang, Yujie Zhou, Jiangmeng Li, Anyi Rao, Hao Sun, Zhiwu Lu, and Ji-Rong Wen. A molecular multimodal foundation model associating molecule graphs with natural language. *CoRR*, abs/2209.05481, 2022.
- [36] Fan-Yun Sun, Jordan Hoffmann, Vikas Verma, and Jian Tang. Infograph: Unsupervised and semi-supervised graph-level representation learning via mutual information maximization. *arXiv preprint arXiv:1908.01000*, 2019.
- [37] Mengying Sun, Jing Xing, Huijun Wang, Bin Chen, and Jiayu Zhou. Mocl: Contrastive learning on molecular graphs with multi-level domain knowledge. *CoRR*, abs/2106.04509, 2021.
- [38] Artur P. Toshev, Gianluca Galletti, Johannes Brandstetter, Stefan Adami, and Nikolaus A. Adams. E(3) equivariant graph neural networks for particle-based fluid mechanics. *CoRR*, abs/2304.00150, 2023.
- [39] Ashish Vaswani, Noam Shazeer, Niki Parmar, Jakob Uszkoreit, Llion Jones, Aidan N Gomez, Łukasz Kaiser, and Illia Polosukhin. Attention is all you need. *Advances in neural information processing systems*, 30, 2017.
- [40] Hongwei Wang, Weijiang Li, Xiaomeng Jin, Kyunghyun Cho, Heng Ji, Jiawei Han, and Martin D. Burke. Chemical-reaction-aware molecule representation learning. In *The Tenth International Conference on Learning Representations, ICLR 2022, Virtual Event, April 25-29, 2022*. OpenReview.net, 2022.
- [41] Ruijia Wang, YiWu Sun, Yujie Luo, Shaochuan Li, Cheng Yang, Xingyi Cheng, Hui Li, Chuan Shi, and Le Song. Injecting multimodal information into rigid protein docking via bi-level optimization. In Alice Oh, Tristan Naumann, Amir Globerson, Kate Saenko, Moritz Hardt, and Sergey Levine, editors, *Advances in Neural Information Processing Systems 36: Annual Conference on Neural Information Processing Systems 2023, NeurIPS 2023, New Orleans, LA, USA, December 10 - 16, 2023*, 2023.
- [42] Yaqing Wang, Abulikemu Abuduweili, Quanming Yao, and Dejing Dou. Property-aware relation networks for few-shot molecular property prediction. In Marc’Aurelio Ranzato, Alina Beygelzimer, Yann N. Dauphin, Percy Liang, and Jennifer Wortman Vaughan, editors, *Advances in Neural Information Processing Systems 34: Annual Conference on Neural Information Processing Systems 2021, NeurIPS 2021, December 6-14, 2021, virtual*, pages 17441–17454, 2021.

- [43] Yuyang Wang, Jianren Wang, Zhonglin Cao, and Amir Barati Farimani. Molclr: Molecular contrastive learning of representations via graph neural networks. *CoRR*, abs/2102.10056, 2021.
- [44] David S. Wishart, Yannick D. Feunang, An Chi Guo, Elvis J. Lo, Ana Marcu, Jason R. Grant, Tanvir Sajed, Daniel Johnson, Carin Li, Zinat Sayeeda, Nazanin Assempour, Ithayavani Iynkkaran, Yifeng Liu, Adam Maciejewski, Nicola Gale, Alex Wilson, Lucy Chin, Ryan Cummings, Diana Le, Allison Pon, Craig Knox, and Michael Wilson. Drugbank 5.0: a major update to the drugbank database for 2018. *Nucleic Acids Res.*, 46(Database-Issue):D1074–D1082, 2018.
- [45] Size Wu, Wenwei Zhang, Sheng Jin, Wentao Liu, ChenChange Loy, Hong Kong, Sensetime Research, and Tetras Ai. Aligning bag of regions for open-vocabulary object detection.
- [46] Zhenqin Wu, Bharath Ramsundar, Evan N Feinberg, Joseph Gomes, Caleb Geniesse, Aneesh S Pappu, Karl Leswing, and Vijay Pande. Moleculenet: a benchmark for molecular machine learning. *Chemical science*, 9(2):513–530, 2018.
- [47] Chaochao Yan, Qianggang Ding, Peilin Zhao, Shuangjia Zheng, Jinyu Yang, Yang Yu, and Junzhou Huang. Retroxpert: Decompose retrosynthesis prediction like a chemist. *Advances in Neural Information Processing Systems*, 33:11248–11258, 2020.
- [48] Shuwen Yang, Ziyao Li, Guojie Song, and Lingsheng Cai. Deep molecular representation learning via fusing physical and chemical information. In Marc’Aurelio Ranzato, Alina Beygelzimer, Yann N. Dauphin, Percy Liang, and Jennifer Wortman Vaughan, editors, *Advances in Neural Information Processing Systems 34: Annual Conference on Neural Information Processing Systems 2021, NeurIPS 2021, December 6-14, 2021, virtual*, pages 16346–16357, 2021.
- [49] Lewei Yao, Jianhua Han, Xiaodan Liang, Dan Xu, Wei Zhang, Zhenguo Li, and Hang Xu. Detclipv2: Scalable open-vocabulary object detection pre-training via word-region alignment.
- [50] Yuning You, Tianlong Chen, Yongduo Sui, Ting Chen, Zhangyang Wang, and Yang Shen. Graph contrastive learning with augmentations. In Hugo Larochelle, Marc’Aurelio Ranzato, Raia Hadsell, Maria-Florina Balcan, and Hsuan-Tien Lin, editors, *Advances in Neural Information Processing Systems 33: Annual Conference on Neural Information Processing Systems 2020, NeurIPS 2020, December 6-12, 2020, virtual*, 2020.
- [51] Daniel Zaharevitz. Aids antiviral screen data, 2015.
- [52] Yuhang Zang, Wei Li, Kaiyang Zhou, Chen Huang, and Chen Change Loy. Open-vocabulary detr with conditional matching. In *European Conference on Computer Vision*, pages 106–122. Springer, 2022.
- [53] Zheni Zeng, Yuan Yao, Zhiyuan Liu, and Maosong Sun. A deep-learning system bridging molecule structure and biomedical text with comprehension comparable to human professionals. *Nature communications*, 13(1):862, 2022.
- [54] Shifeng Zhang, Cheng Chi, Yongqiang Yao, Zhen Lei, and Stan Z. Li. Bridging the gap between anchor-based and anchor-free detection via adaptive training sample selection. In *2020 IEEE/CVF Conference on Computer Vision and Pattern Recognition (CVPR)*, Jun 2020.
- [55] Zaixi Zhang, Qi Liu, Hao Wang, Chengqiang Lu, and Chee-Kong Lee. Motif-based graph self-supervised learning for molecular property prediction.
- [56] Haiteng Zhao, Shengchao Liu, Chang Ma, Hannan Xu, Jie Fu, Zhihong Deng, Lingpeng Kong, and Qi Liu. GIMLET: A unified graph-text model for instruction-based molecule zero-shot learning. In Alice Oh, Tristan Naumann, Amir Globerson, Kate Saenko, Moritz Hardt, and Sergey Levine, editors, *Advances in Neural Information Processing Systems 36: Annual Conference on Neural Information Processing Systems 2023, NeurIPS 2023, New Orleans, LA, USA, December 10 - 16, 2023*, 2023.

A Related Work

Molecular Learning Based on Graphs. Molecular graphs are commonly employed as inputs for molecular learning. Numerous studies employ various GNNs as base encoders to facilitate molecular representation learning for downstream tasks [48, 42]. These approaches generally require supervised signals and are not applicable to other tasks. Recent advancements in research have introduced self-supervised learning methods. Some methods focus on reconstruction tasks for pre-training. PreGNN [13] enhances GNN pre-training through context prediction and node/edge attribute masking. GROVER [33] introduces molecular-specific self-supervised techniques, including contextual property prediction and graph-level motif prediction. MGSSL [55] adopts a motif-based graph self-supervised strategy that predicts the topology and labels of motifs. Additionally, some methods leverage contrastive learning for pertaining, and general graph augmentation methods [50] are also applicable to molecular datasets. InfoGraph [36] optimizes model training by maximizing the mutual information between the global graph representations and their substructures of varying granularity. Incorporating chemical domain knowledge, MoCL [37] employs two novel molecular graph augmentation methods: replacing specific substructures or altering a few carbon atoms. MolR [40] aims to maintain the equivalence relation between reactants and products within the embedding space. Despite the effectiveness of pre-trained models, it is still challenging to generalize new categories or tasks without labeled examples or fine-tuning.

Fine-grained Vision-Language models. Various works design fine-grained alignment methods to better align the region visual features (RoIs) into text features of the vision-language model (VLM). OV-DETR [52] introduces a transformer-based approach for open vocabulary object detection, using conditional binary matching instead of traditional bipartite matching. VLDet [23] aligns objects and language by transforming images into regions and captions into words, employing a set matching strategy. DetCLIPv2 [49] leverages ATSS [54] for object detection, trained on a standard detection dataset, a grounding dataset, and an image-text pairs dataset. BARON [45] aligns embeddings within groups of related regions, processing them through a text encoder. CoDet [28] treats region-word alignment as a co-occurring object discovery problem. F-VLM [19] uses a CLIP vision encoder and a VLM feature pooler for region features, combining detection scores with VLM predictions. RO-ViT [15] addresses positional embedding gaps in vision-language pre-training by introducing a cropped positional embedding module, enhancing alignment for downstream tasks. While these methods rely on a detection model to assign labels to the RoI, our approach lacks such a model to provide supervised signals for motifs, making it challenging to align fine-grained information.

B Technical Details of Text-based Molecule Editing Task

Following the molecule editing framework proposed by [26], we utilize FineMolTex and the generation module, including an encoder and a decoder, to generate molecules. This process is structured into two phases. The first phase is the space alignment, which utilizes two projectors, p_m and p_g , to align the representation space of the generative model with our model into a joint representation space following a contrastive learning strategy as:

$$L_{\text{ali}} = -\frac{1}{2}\mathbb{E}_m[\log \frac{\exp(\cos(\mathbf{z}_{\mathbf{m}_0}, p_g(\mathbf{w}))/\tau)}{\exp(\cos(\mathbf{z}_{\mathbf{m}_0}, p_g(\mathbf{w}))/\tau) + \sum_{w'} \exp(\cos(\mathbf{z}_{\mathbf{m}_0}, p_g(\mathbf{w}'))/\tau)} + \log \frac{\exp(\cos(w, p_m(\mathbf{z}_{\mathbf{m}_0}))/\tau)}{\exp(\cos(\mathbf{w}, p_m(\mathbf{z}_{\mathbf{m}_0}))/\tau) + \sum_{\mathbf{z}_{\mathbf{m}'_0}} \exp(\cos(\mathbf{w}, p_m(\mathbf{z}_{\mathbf{m}'_0}))/\tau)}], \quad (11)$$

where m is the molecule, $\mathbf{z}_{\mathbf{m}_0}$ denotes the embedding generated by our model, \mathbf{w} is the embedding produced by the encoder of the generation model, $\mathbf{z}_{\mathbf{m}'_0}$ and w' are the embeddings of negative samples sampled from the same batch.

The second phase is latent optimization. We directly learn the latent embedding \mathbf{w}^* , ensuring it remains closely aligned with the initial molecular embedding while also resembling the embedding of the text prompt. We employ two similarity scores as the objective function. To ensure that the generated molecule is similar to the text prompt, we utilize the projector to transform the latent embedding of the molecule into the joint representation space, and then calculate its cosine similarity with the embedding of text $\mathbf{z}_{\mathbf{t}_0}$. To ensure the generated molecule is also similar to the initial molecule, we compute the l_2 distance between \mathbf{w}^* and the initial embedding \mathbf{w} .

$$\mathbf{w}^* = \operatorname{argmin}_{\mathbf{w}^*} (\cos(p_g(\mathbf{w}^*), \mathbf{z}_{t_0})/\tau) + \lambda l_2(\mathbf{w}^*, \mathbf{w}). \quad (12)$$

Given the optimized latent embedding \mathbf{w}^* , the decoder of the generation module can get the output molecules. For the four prompts aimed at generating molecules with specific motifs, we excluded molecules from the dataset that already contained these motifs.

C Reproducibility Information

C.1 Dataset Statistics

C.1.1 Pre-training Dataset

We employ a dataset known as PubChemSTM [26], derived from the PubChem database [16], which consists of chemical structure-text pairs. The dataset is available in two versions: PubChemSTM-raw, which retains the original annotations, and PubChemSTM-extracted, where the names of the molecules are replaced with the generic term "this molecule". In our study, we use the PubChemSTM-extracted version. Examples of PubChemSTM-extracted are illustrated in Figure 6.

C.1.2 Retrieval Datasets

We utilize three pertinent fields from the DrugBank database [44] for each small molecule drug in our zero-shot retrieval task: the Description field, the Pharmacodynamics field, and the Anatomical Therapeutic Chemical (ATC) classification. Specifically, the DrugBank-Description provides a comprehensive overview of the drug’s chemical characteristics, historical development, and regulatory status. The DrugBank-Pharmacodynamics section details the mechanisms through which the drug influences or alters the organism in which it is used. This includes both desired and undesired effects (commonly referred to as side effects). Lastly, the DrugBank-ATC classification system organizes the molecules into groups based on the organs or systems they target, along with their therapeutic, pharmacological, and chemical properties. The datasets consist of 1154, 1005, and 3007 molecule-text pairs for each field, respectively.

C.1.3 Molecule Property Prediction Datasets

The MoleculeNet dataset, used for molecular property prediction in downstream tasks, contains two main categories. Some datasets are used for pharmacological property prediction. The Blood-Brain Barrier Penetration (BBBP) [30] dataset evaluates whether a molecule can penetrate the central nervous system. The three datasets related to toxicity—Tox21 [5], ToxCast [46], and ClinTox [10]—assess the toxicity of molecular compounds. The Side Effect Resource (SIDER) [18] dataset contains information on adverse drug reactions from a marketed drug database. Other datasets are used for biophysical property prediction. The Maximum Unbiased Validation (MUV) [32] dataset, a subset of the PubChem BioAssay (PCBA), is created using a refined nearest neighbor analysis. The HIV dataset, sourced from the Drug Therapeutics Program (DTP) AIDS Antiviral Screen [51], focuses on predicting the inhibition of HIV replication. The BACE dataset, included in MoleculeNet [46], measures the binding affinity of various inhibitors to β -secretase 1 (BACE-1). The overall dataset statistics of MoleculeNet are shown in Table 5.

Table 5: Dataset statistics of MoleculeNet for molecule property prediction task.

Dataset	Tasks	Molecules
BBBP	1	2,039
Tox21	12	7,831
ToxCast	617	8,576
Sider	27	1,427
ClinTox	2	1,478
MUV	17	93,087
HIV	1	41,127
Bace	1	1,513

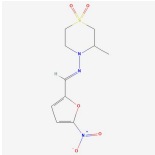
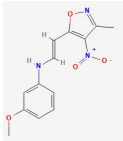
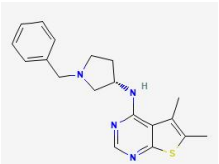
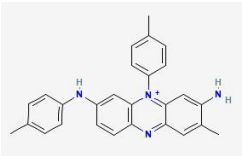
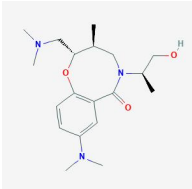
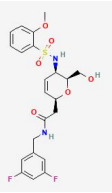
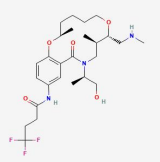
Molecular Graphs	Descriptions
	This molecule is a nitrofurantoin antimicrobial agent used to treat Chagas disease (American trypanosomiasis), a chronic protozoal infection due to <i>Trypanosoma cruzi</i> that can lead to severe disability and death from gastrointestinal and cardiac disease. This molecule is rarely associated with serum aminotransferase elevations during therapy and has not been linked to cases of clinically apparent liver injury.
	This molecule is a substituted aniline and an aromatic ether.
	This molecule is an N-(1-benzylpyrrolidin-3-yl)-5,6-dimethylthieno[2,3-d]pyrimidin-4-amine in which the chiral centre has S configuration. Both enantiomers act as fatty acid synthase inhibitors, although the (S)-enantiomer was found to be more than 4 times as active as the (R)-enantiomer. It has a role as a fatty acid synthesis inhibitor and an EC 2.3.1.85 (fatty acid synthase) inhibitor. It is an enantiomer of a (R)-Fasnall
	This molecule is an organic cation consisting of 7-(4-methylanilino)phenazine carrying additional methyl, amino and 4-methylphenyl substituents at positions 2, 3 and 5 respectively. One of four components of mauvaine, a synthetic violet-coloured dye. It has a role as a histological dye. It is an organic cation and a member of phenazines.
	This molecule is a tertiary amino compound and a dialkylarylamine.
	This molecule is a sulfonamide.
	This molecule is a lactam and an azamacrocycle.

Figure 6: Examples on PubChemSTM-extracted

C.2 Baselines

The publicly available implementations of Baselines can be found at the following URLs:

- KV-PLM (MIT license): <https://github.com/thunlp/KV-PLM>
- MoleculeSTM (MIT license): <https://github.com/chao1224/MoleculeSTM>
- MoMu-K and Momu-S (MIT license): <https://github.com/ddz16/MoMu>
- MolCA (MIT license): <https://github.com/acharkq/MolCA>
- AttrMasking (MIT license): <https://github.com/snap-stanford/pretrain-gnns/>
- ContextPred (MIT license): <https://github.com/snap-stanford/pretrain-gnns>
- InfoGraph (MIT license): <https://github.com/sunfanyunn/InfoGraph>
- MolCLR (MIT license): <https://github.com/yuyangw/MolCLR>
- GraphMVP (MIT license): <https://github.com/chao1224/GraphMVP>

C.3 Operating Environment

- Operating system: Linux ubuntu 5.15.0-102-generic.
- CPU information: Intel(R) Xeon(R) Platinum 8358 CPU @2.60GHz.
- GPU information: NVIDIA A800 80GB.

C.4 Implementation Details

We use Pytorch to implement our model. For the pre-trained baselines, we directly utilize the checkpoints provided by the authors. For other baselines, we utilize the original codes from their authors and train the models in an end-to-end way. We utilize the BRICS [6] to fragment molecules into motifs. As BRICS primarily cleaves bonds according to a predefined set of chemical reactions, often resulting in several large fragments per molecule, we further utilize the post-processing procedure proposed by MGSSL [55], which is designed to minimize the number of ring variants and facilitate the cleavage of side chains. Subsequently, we build a vocabulary of all motif tokens identified in the PubChemSTM dataset, which comprises a total of 30,080 unique motifs. We note that within our dataset, certain motifs are infrequently present, while others are prevalent but lack significant semantic value. This uneven distribution presents a challenge for the model, as it struggles to extract meaningful insights from such disparate occurrences. Thus we have constructed a masking set of 2,457 motifs that excludes motifs appearing fewer than 8 times or more than 80,005 times. Based on this masking set, we selectively mask motifs to enhance the model’s learning efficiency and focus on extracting valuable information from the most informative tokens. To map the embedding of the molecule and the text into the same dimension, we further utilize a projector MLP layer for the graph encoder. We utilize Adam as the optimizer for the GNN encoder, the language model, the two projector MLPs, the multi-modal framework, and the motif classifier with different learning rates, and test the learning rate ranging from $\{1e-3, 1e-4, 1e-5\}$. We set $\ell = 2$, and test ℓ_{trm_M} ranging from $\{1, 2, 3, 4, 5\}$, ℓ_{trm_T} ranging from $\{8, 10, 12\}$. For the coefficient of loss function, we test α and β ranging from $\{0.5, 1, 2\}$. We train our model with a total batch size of 16 for 15 epochs. For fair comparisons, we randomly run 5 times and report the average results for all methods.

Optimal Parameters. The optimal parameters can be found in the config.json file in our code repository. Specifically, we set the dimension of the graph encoder to 300 and the dimensions of the transformer and cross-attention layer to 768. The hyperparameters are set as $\alpha = 0.5$ and $\beta = 1$. For $\ell = 2$, we set ℓ_{trm_M} to 2 for the first round and 3 for the second round, and ℓ_{trm_T} to 10 for the first round and 12 for the second round. The learning rates are set as follows: $1e-5$ for the graph encoder, text encoder, transformer layers, and cross-attention layer; $3e-5$ for the projector MLP of the graph encoder; and $1e-3$ for the motif classifier.

Table 6: Accuracy ($\% \pm \sigma$) of graph-text retrieval task on DrugBank-Description.

T	Given Molecular Graph			Given Text		
	4	10	20	4	10	20
KV-PLM	73.80 \pm 0.00	53.96 \pm 0.29	40.07 \pm 0.38	72.86 \pm 0.00	52.55 \pm 0.29	40.33 \pm 0.00
MolCA	93.75 \pm 0.09	87.25 \pm 0.06	82.77 \pm 0.12	90.71 \pm 0.04	84.97 \pm 0.16	77.53 \pm 0.15
MoMu-S	76.52 \pm 0.12	61.66 \pm 0.25	50.00 \pm 0.08	77.62 \pm 0.06	61.49 \pm 0.15	52.20 \pm 0.13
MoMu-K	74.15 \pm 0.08	57.18 \pm 0.16	47.97 \pm 0.14	77.79 \pm 0.12	62.33 \pm 0.18	47.97 \pm 0.06
MoleculeSTM	99.15 \pm 0.00	97.19 \pm 0.00	95.66 \pm 0.00	99.05 \pm 0.37	97.50 \pm 0.46	95.71 \pm 0.46
FineMolTex	99.58\pm0.05	97.97\pm0.00	96.45\pm0.16	99.58\pm0.04	97.89\pm0.08	96.11\pm0.12

D Additional Results

D.1 Graph-text Retrieval Task on Drugbank-Description

The results of the graph-text retrieval task on Drugbank-Description can be found in Table 6. We can observe that our model consistently performs better than baselines.

D.2 Visual Analysis of the Output Molecules on 4 Text-based Molecule Editing Tasks

We present additional visual analyses of the output molecules for four text-based molecule editing tasks, as depicted in Figure 8. FineMolTex effectively generates motifs that align with expectations, demonstrating its superior ability to learn fine-grained knowledge.

D.3 Visualization of Motif and Word Tokens with Legends

Figure 7 displays the complete visualization with legends, illustrating that the embeddings of relevant motifs and words are closer in the embedding space.

D.4 Explanation of Predictions on Masked Motifs Based on Word Tokens

We provide additional explanations for the predictions of FineMolTex in Figure 9, verifying whether the words with the highest interpretive weights are relevant to the masked motifs. In (1), "indanone" is directly the name of the masked motif. In (2), the masked motif is part of "azobenzene". In (3), "azetidine" is part of the masked motif. In (4), the masked motif is a substructure of "trimethylamino" and "butyrobetaine". These explanations demonstrate that FineMolTex has learned fine-grained knowledge, providing insights for the prediction task.

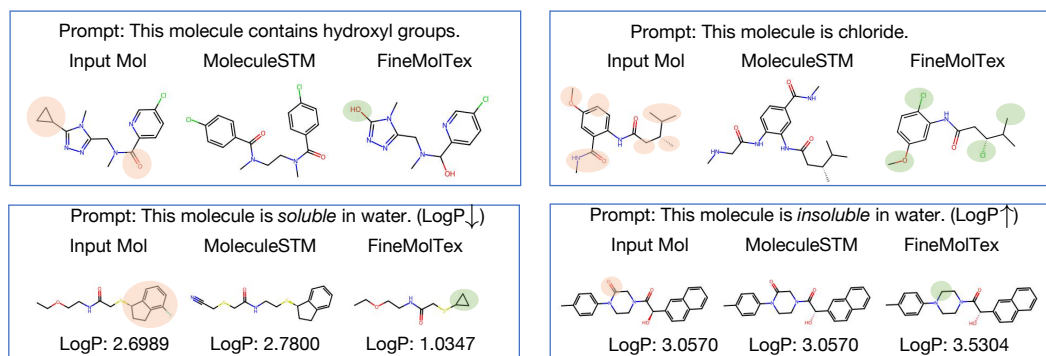


Figure 8: Additional visual analysis of the output molecules of MoleculeSTM and Motif-MolTex on 4 text-based molecule editing tasks. Differences between the input molecule and output molecule of FineMolTex are highlighted in red and green circles. Higher LogP indicates lower water solubility.

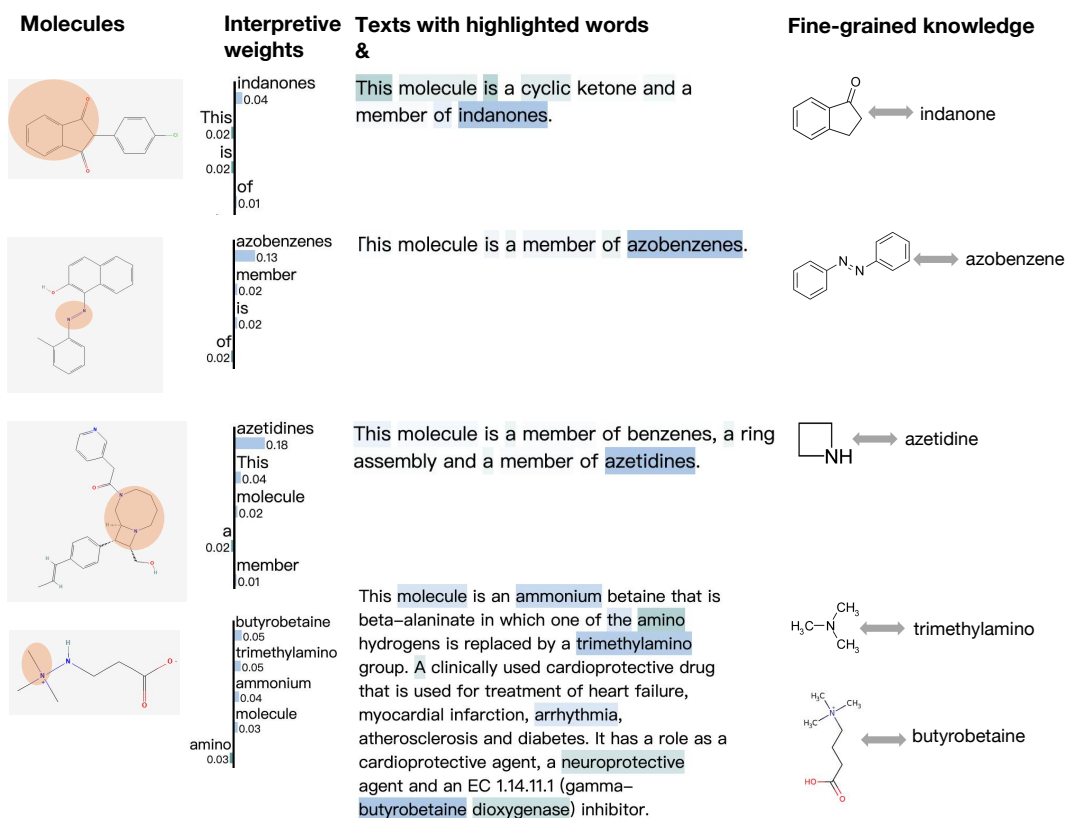


Figure 9: Explanations of prediction of motifs based on word tokens.